

Delays in Spiking Neural Networks: A State Space Model Approach

Sanja Karilanova, Subhrakanti Dey, and Ayça Özçelikkale

Department of Electrical Engineering, Uppsala University, Sweden
{Sanja.Karilanova, Subhrakanti.Dey, Ayca.Ozcelikkale}@angstrom.uu.se}

Abstract. Spiking neural networks (SNNs) are biologically inspired, event-driven models suited for temporal data processing and energy-efficient neuromorphic computing. In SNNs, richer neuronal dynamic allows capturing more complex temporal dependencies, with delays playing a crucial role by allowing past inputs to directly influence present spiking behavior. We propose a general framework for incorporating delays into SNNs through additional state variables. The proposed mechanism enables each neuron to access a finite temporal input history. The framework is agnostic to neuron models and hence can be seamlessly integrated into standard spiking neuron models such as Leaky Integrate-and-Fire (LIF) and Adaptive LIF (adLIF). We analyze how the duration of the delays and the learnable parameters associated with them affect the performance. We investigate the trade-offs in the network architecture due to additional state variables introduced by the delay mechanism. Experiments on the Spiking Heidelberg Digits (SHD) dataset show that the proposed mechanism matches existing delay-based SNNs in performance while remaining computationally efficient, with particular gains in smaller networks. Code available at <https://github.com/sannkka/Modeling-State-Delays-in-SNNs>.

Keywords: spiking neural networks (SNN) · state-space models (SSM) · neuromorphic · delays · memory

1 Introduction

Spiking Neural Networks (SNNs) have emerged as a more biologically plausible class of neural models compared to conventional artificial neural networks (ANNs), offering promising advantages in temporal processing and energy efficiency, particularly when deployed on neuromorphic hardware [6]. SNNs encode information in the timing of discrete spikes, allowing them to capture temporal structure and making them well suited for modeling time-dependent signals such as audio [1], or visual patterns [13]. Despite these advantages, achieving performance comparable to that of ANNs remains an open challenge, in part due to the limited temporal expressivity of current SNN models.

In biological neural systems, temporal delays play a critical computational role. Delays that enable neurons to integrate information from multiple past

moments support tasks such as hearing [3] and brain activity [4]. Inspired by these findings, numerous works have explored incorporating delays into computational SNNs models. Theoretical analyses have shown that an SNN with k adjustable delays can compute a much richer class of functions than a threshold circuit with k adjustable weights [24]. Empirical studies have also demonstrated improved performance when optimizing spike transmission delays along with synaptic weights or membrane time constants [7, 32]. These results suggest that delays can enrich the information processing capabilities of SNNs and their internal representation. However, despite these promising results, practical methods for introducing structured, scalable, and differentiable forms of delay into modern deep SNNs remains an ongoing research problem.

In this work, we propose a method based on State Space Models (SSMs) for equipping SNNs with delays. The method uses a time-shift based state transition, which enables each neuron to access both its current input and the most recent history of past input values. The formulation is general and can be incorporated into arbitrary spiking neuron models, such as Leaky Integrate-and-Fire (LIF) and Adaptive LIF (adLIF) and their recurrent variant Recurrent LIF (RLIF) and Recurrent adLIF (RadLIF) [1]. Conceptually, the framework bridges ideas from SSMs and SNNs, allowing SNNs to capture a fixed number of past inputs in a structured and interpretable manner.

Our contributions can be summarized as follows:

- We propose incorporating delays within the neuron state dynamics via additional delay variables, enabling access to a finite temporal history of inputs.
- The formulation is general and easily integrable into existing spiking neuron models, including LIF, RLIF, adLIF, and RadLIF.
- We systematically analyze delay order (number of accessible past inputs) and associated learnable parameters, studying trade-offs between network size and delay order.
- The framework introduces either no additional trainable parameters (non-trainable case) or a parameter count comparable to other SNN delay models.

The proposed models achieve performance comparable to existing delay-based SNN approaches on the Spiking Heidelberg Digits (SHD) dataset. The observed trade-offs highlight promising directions for future exploration, particularly showing that incorporating delays can substantially improve accuracy in smaller SNNs where the neuron count limits temporal capacity.

2 Related Work

In the SNN literature, three main types of delays are commonly modeled: axonal delays, applied to the output of a neuron [31–33]; dendritic delays, applied to its input [8]; and synaptic delays, specific to each connection between neuron pairs [7, 9, 14, 17]. In contrast to these formulations, we propose an SSM based approach where delays are modeled within the state dynamics of the neuron. See Figure 1 for a schematic illustration.

A typical approach for modeling delays in SNNs is through explicit temporal convolutions applied to spike trains [17, eqn. 6–8], [33, eqn. 4], [31, eqn. 3], where a kernel with a relatively small number of nonzero weights is convolved with the spike train, and the relative positions of the non-zero weights encode the delay mechanism. A related approach, and the one closest to our proposed method, is to incorporate temporal buffer directly into the neuron state as an explicit finite memory of past inputs [34]. Given that linear state-space models may be interpreted as temporal convolutions [12], this type of approaches can be seen as an extra incorporation of delay into temporal convolution, see also (3). An alternative line of work models delays as continuous-valued spike-time shifts [16, 25], which permits exact gradient methods but is less compatible with discrete surrogate-gradient training pipelines.

The role of delays in SNNs has been studied from various perspectives including jointly training weights and delays [7], learning only delays [14], exploring heterogeneous delays and their relation to weight-precision requirements [32], and investigating their role in temporal hierarchies across layers [26]. Learning algorithms for delays range from BPTT [17, 31] and STDP [9] to exact spike-time gradients [16, 25]. Our formulation represents delays as state variables, making it compatible with BPTT and the widely used surrogate-gradient method for training SNNs [27].

Delays have long been studied in fields such as signal processing and control theory. In discrete-time dynamical systems, they are typically modeled through delay-difference and state-space formulations [28, 30]. Modern deep SSMs, which stack multiple state-space layers combined with nonlinearities, have demonstrated strong performance in sequence modeling tasks [15]. Subsequent work introduced parameterization in deep SSMs, which effectively captures delayed state dependencies [11, 36]. In parallel, hybrid approaches have emerged that bridge SNNs and SSMs, combining properties and capabilities from both models [10, 19–21, 32, 35]. We build on this line of work and adopt the SSM perspective on delay modeling within spiking neural architectures. This allows SNNs to incorporate structured temporal dependencies through a principled state-space formulation.

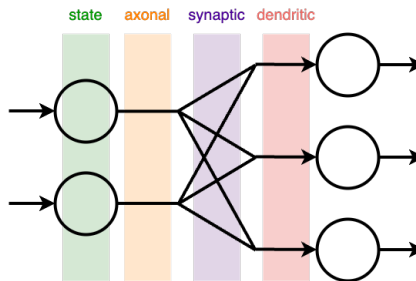


Fig. 1: Delay modeling approaches. Proposed method: delays within neuron state dynamics (green). Figure inspired by [16, Fig. 3(a)].

3 Methods

3.1 Preliminaries

General Spiking Neuron Model A single general feed-forward discrete-time n -state dimensional spiking neuron can be defined as [21]:

$$\mathbf{v}_s[t+1] = \mathbf{A}_s \mathbf{v}_s[t] + \mathbf{B}_s i_s[t] - \mathbf{R}s[t] \quad (1a)$$

$$s[t] = f_{\Theta}(\mathbf{v}_s[t]) = \begin{cases} 1 & \text{if } \mathbf{v}_s[t] \in \Theta \\ 0 & \text{otherwise} \end{cases} \quad (1b)$$

where $i_s[t] \in \mathbb{R}^{1 \times 1}$ is the input to the neuron, $s[t] \in \mathbb{R}^{1 \times 1}$ is the output of the neuron and $\mathbf{v}_s \in \mathbb{R}^{n_s \times 1}$ is the state variable of the neuron. The matrices $\mathbf{A}_s \in \mathbb{R}^{n_s \times n_s}$, $\mathbf{B}_s \in \mathbb{R}^{n_s \times 1}$, $\mathbf{R} \in \mathbb{R}^{n_s \times 1}$ represents the leak, impact of the input and the reset feedback, respectively. The spiking behavior is described by $f_{\Theta}(\cdot)$, where the neuron spikes when the state enters into the region described by Θ .

The model in (1) generalizes commonly used formulations including including the Leaky Integrate-and-Fire (LIF) and adaptive LIF (adLIF) neurons and their recurrent variants Recurrent LIF (RLIF) and Recurrent adLIF (RadLIF) [21].

In SNNs, output spikes from the pre-synaptic layer ($l-1$) serve as inputs to the post-synaptic layer (l). Let $\mathbf{W} \in \mathbb{R}^{L_{\text{post}} \times L_{\text{pre}}}$ and $\mathbf{V} \in \mathbb{R}^{L_{\text{post}} \times L_{\text{post}}}$ be the feedforward and recurrent weight matrices, with L_{pre} , L_{post} the layer sizes. The input current is $\mathbf{i}[t] = \mathbf{W} \times \mathbf{s}^{l-1}[t] + \mathbf{V} \times \mathbf{s}^l[t]$, where $\mathbf{s}^{l-1}[t]$ and $\mathbf{s}^l[t]$ are spike vectors from the previous and current layer.

Linear State Space Model A discrete-time time-invariant linear SSM can be written as [15]:

$$\mathbf{v}_d[t+1] = \mathbf{A}_d \mathbf{v}_d[t] + \mathbf{B}_d i_d[t] \quad (2a)$$

$$\mathbf{y}_d[t] = \mathbf{C}_d \mathbf{v}_d[t] + \mathbf{D}_d i_d[t], \quad (2b)$$

where $\mathbf{v}_d[t]$, $i_d[t]$, $\mathbf{y}_d[t]$ denote the state vector, the input vector, and the output vector, respectively. Here, the state transition matrix $\mathbf{A}_d \in \mathbb{R}^{n_d \times n_d}$ describes the internal recurrent behavior of SSM. The matrices $\mathbf{B}_d \in \mathbb{R}^{n_d \times 1}$, $\mathbf{C}_d \in \mathbb{R}^{n_{\text{out}} \times n_d}$, $\mathbf{D}_d \in \mathbb{R}^{n_{\text{out}} \times 1}$ describe the interaction of the SSM through its inputs and outputs.

Temporal Convolution Representation of Linear SSM A key property of linear SSMs is that it can be expressed as a causal temporal convolution. Under the initial condition $\mathbf{v}_d[t] = 0$, for $t \leq 0$, unrolling the recurrence in (2a) yields

$$\mathbf{v}_d[t] = \sum_{k=0}^{t-1} \mathbf{A}_d^k \mathbf{B}_d i_d[t-k]. \quad (3)$$

The state variable at time t is therefore a convolution of the input with the kernel $d[t] = \mathbf{A}_d^t \mathbf{B}_d$ i.e. $\mathbf{v}_d[t] = d[t] * i_d[t]$, where $*$ denotes convolution.

Linear SSM with Time Shift State Transition Matrix The lower shift matrix is a structured matrix whose nonzero entries lie only on the subdiagonal. Let \mathbf{A}_d in (2) denote such a matrix i.e. let

$$\mathbf{A}_d = \begin{bmatrix} 0 & 0 & \dots & 0 & 0 \\ a_1 & 0 & \dots & 0 & 0 \\ 0 & a_2 & \dots & 0 & 0 \\ \vdots & \ddots & \vdots & \vdots & \vdots \\ 0 & 0 & \dots & a_{n_d-1} & 0 \end{bmatrix} \text{ i.e., } [\mathbf{A}_d]_{i,j} = \begin{cases} a_j & \text{for } i-1 = j \\ 0 & \text{otherwise} \end{cases} \quad (4a)$$

where $[\mathbf{A}_d]_{i,j}$ denotes the (i, j) -th entry of \mathbf{A}_d , and let $\mathbf{B}_d = [1, 0, \dots, 0]^T$. Although the parameters a_i are free in general, in this paper we set $a_i = 1$ for all i . Under this choice, and following (3), \mathbf{v}_d reduces to a simple temporal memory of the last n inputs (a shift register), i.e.,

$$\mathbf{v}_d[t] = [i_d[t], i_d[t-1], i_d[t-2], \dots, i_d[t-n_d+1]]^T, \quad (5)$$

see Appendix A.2 for a demonstration.

3.2 Proposed Model

Let \mathbf{v}_s be the state variable of the general spiking neuron in (1) with parameter matrices $\mathbf{A}_s, \mathbf{B}_s, \mathbf{C}_s$ and state dimension n_s . Let \mathbf{v}_d be the state variable of the time-shift SSM in Section 3.1 with parameter matrices $\mathbf{A}_d, \mathbf{B}_d, \mathbf{C}_d$ and state dimension n_d . Our proposed spiking neuron model with state-delays is defined as:

$$\mathbf{v}_d[t+1] = \mathbf{A}_d \mathbf{v}_d[t] + \mathbf{B}_d i_d[t] \quad (6a)$$

$$\mathbf{v}_s[t+1] = \mathbf{A}_s \mathbf{v}_s[t] + \mathbf{B}_s i_s[t] + \mathbf{A}_{sd} \mathbf{v}_d[t] - \mathbf{R}s[t] \quad (6b)$$

$$s[t] = f_{\Theta}(\mathbf{C}_s \mathbf{v}_s[t] + \mathbf{C}_d \mathbf{v}_d[t]) = \begin{cases} 1 & \text{if } (\mathbf{C}_s \mathbf{v}_s[t] + \mathbf{C}_d \mathbf{v}_d[t]) \in \Theta \\ 0 & \text{otherwise} \end{cases} \quad (6c)$$

Here, $\mathbf{A}_{sd} \in \mathbb{R}^{n_s \times n_d}$ denotes the parameters that delayed inputs in the state \mathbf{v}_d are multiplied with before they are added to the neuron state \mathbf{v}_s .

The above equations present a spiking neuron with additional access to temporal memory through the state variable $\mathbf{v}_d[t]$. The state dimension n_d defines the maximum order of the delays provided to the spiking neuron i.e. the number of directly accessible past quantities. The input i_s to \mathbf{v}_s , as defined in Section 3.1, represents the input spikes to the neuron. The input i_d to \mathbf{v}_d represents the input stored in the temporal memory. See Table 1 for an overview of the notation. Examples of the proposed models with LIF, RLIF, adLIF and RadLIF neuron models are provided in Appendix A.1. A high-level visualization of the proposed model is presented in Figure 2.

3.3 Delay parameters

We now provide an overview of all parameters related to the additional delay variable \mathbf{v}_d in (6). We have \mathbf{A}_d and \mathbf{B}_d as in Section 3.1, hence they are fixed

Table 1: Table of notation.

Notation	Meaning
$\mathbf{v}_s[t]$	State of the neuron’s intrinsic components
$\mathbf{v}_d[t]$	State of the neuron’s delay component
n_s	Dimension of \mathbf{v}_s
n_d	Dimension of \mathbf{v}_d (delay order)
$\mathbf{A}_s, \mathbf{B}_s, \mathbf{C}_s$	Linear model parameters of \mathbf{v}_s
$\mathbf{A}_d, \mathbf{B}_d, \mathbf{C}_d$	Linear model parameters of \mathbf{v}_d
\mathbf{R}	Reset parameters
\mathbf{A}_{sd}	Delay parameters
$i_s[t]$	Input to \mathbf{v}_s
$i_d[t]$	Input to \mathbf{v}_d
$s[t]$	Spike output of the neuron
l	Number of hidden layers
h	Number of neurons in a hidden layer

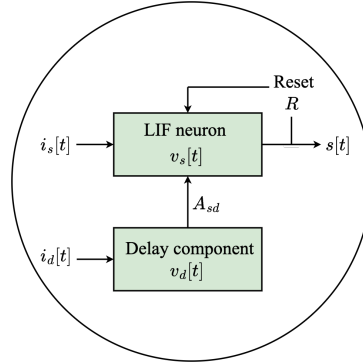


Fig. 2: Proposed delay component incorporated into SNN neuron model (LIF).

and non-trainable. Under LIF/RLIF/adLIF/RadLIF neuron models (see Appendix A.1), we do not use \mathbf{C}_d . Hence, the only additional (possibly trainable) parameter is \mathbf{A}_{sd} . In the rest of this section, we focus on \mathbf{A}_{sd} .

The parameter matrix \mathbf{A}_{sd} determines how the delay variable \mathbf{v}_d contributes to the intrinsic neuron state \mathbf{v}_s in (6). We consider four settings for its elements:

- $\mathbf{A}_{sd} = \text{Ones}$, where $[\mathbf{A}_{sd}]_{ij} = 1$
- $\mathbf{A}_{sd} = \text{Linear decay}$, where $[\mathbf{A}_{sd}]_{ij} = (n_d - j) \frac{1}{n_d}$
- $\mathbf{A}_{sd} = \text{Exponential decay}$, where $[\mathbf{A}_{sd}]_{ij} = e^{-0.5j}$
- $\mathbf{A}_{sd} \sim \text{Uniform distribution}$, where $[\mathbf{A}_{sd}]_{ij} \sim U(0, 1)$

The equal sign = is used in the cases where the elements of \mathbf{A}_{sd} are deterministic, while the sign \sim is used in the case where the elements of \mathbf{A}_{sd} are randomly drawn from a distribution. The matrix of delay parameters \mathbf{A}_{sd} can be trainable or fixed. When it is fixed, its elements do not change during the training of the SNN and remain as initially set. When it is trainable, the initial set values of \mathbf{A}_{sd} represent their initialization, and they change during the training phase without the constraint of preserving the distribution their initialization had, i.e., for instance if $[\mathbf{A}_{sd}]_{ij}$ is initialized as ‘Ones’, the parameters do not stay all ones or all equal. In Section 5 we distinguish these cases by stating whether \mathbf{A}_{sd} is non-trainable or trainable.

Due to our parameter choices in Section 3.1, the delay variable $\mathbf{v}_d[t]$ is simply a vector containing the past n_d scalar inputs $i_d[t]$, see (5). Consequently, the delay contribution $\mathbf{A}_{sd}\mathbf{v}_d[t]$ corresponds to a weighted combination of the past n_d inputs $i_d[t]$ (see Figure 4 in Appendix A.3 for illustration), i.e.,

$$\mathbf{A}_{sd}\mathbf{v}_d[t] = [\mathbf{A}_{sd}]_0 i_d[t] + [\mathbf{A}_{sd}]_1 i_d[t-1] + \dots + [\mathbf{A}_{sd}]_{n_d-1} i_d[t-n_d+1]. \quad (7)$$

Figure 3 illustrates how the coefficients $[\mathbf{A}_{sd}]_i$ appear under the four settings described above.

3.4 Computational complexity

The proposed neuron model with delays, given in (6), extends the baseline formulation in (1) by introducing an additional state variable \mathbf{v}_d and its associated

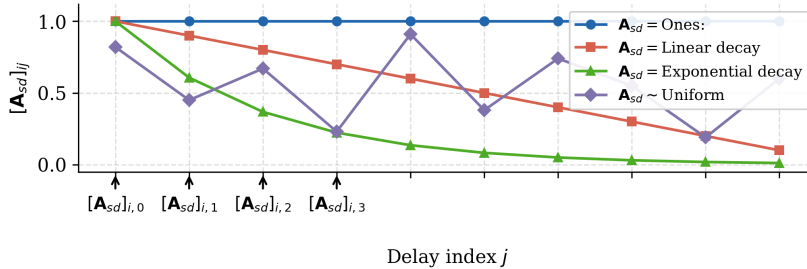


Fig. 3: Visualization of the different parameter settings explored for the elements of A_{sd} . For $[A_{sd}]_{ij} \sim \text{Uniform}$, one random instance is shown as an example.

parameters A_d , B_d , A_{sd} , and C_d . The dimensionality of these matrices is determined by the delay order n_d . In this section, we analyze how this additional state and its parameters influence the computational complexity of the spiking neuron for the case of LIF and adLIF neuron as defined in Appendix A.1.

Number of trainable parameters The baseline definition of the LIF neuron model has 1 trainable parameter, i.e., α , while the adLIF neuron model has 4 trainable parameters, i.e., α, β, a, b . Let l be the number of hidden layers, each with h neurons, and let c_{in} and c_{out} be the number of input and output channels to the network. The trainable parameter counts for each network component are:

- feedforward synaptic connections: $c_{in}h + h^2(l - 1) + hc_{out}$
- recurrent synaptic connections: $l(h^2 - h)$
- neuron parameters: lh for LIF and $4lh$ for adLIF
- normalization layers: $2(hl + c_{out})$
- delays: n_dhl if A_{sd} trainable, 0 otherwise.

From the above calculations, the delay mechanism introduces approx. n_dhl additional parameters, but only if the matrix A_{sd} is trainable. **If A_{sd} is non-trainable, the number of trainable parameters does not increase i.e. it is equal to the number of trainable parameters of the neuron without delays.** Even when A_{sd} is trainable, the number of delay-related parameters is small compared to the number of synaptic connections, which scale as h^2 . Relatively small values of n_d already achieve competitive performance (see Section 5). Hence, since h is expected to be chosen as much larger than both n_d and l in LIF and adLIF networks, the additional computational and parametric overhead from incorporating delays is typically negligible.

We now compare the number of trainable parameters introduced by our delay formulation with those reported in related work.

In [7, Table 1], introducing delays increased the parameter count from 38.7k to 75.8k, i.e., by 37.1k parameters. For the same architecture, our approach increases the number of parameters by $n_dhl = n_d \times 128 \times 2$. For $n_d = 10$, this corresponds to about 2.6k parameters, an order of magnitude smaller than in [7].

In [32, Section 2.1], each neuron learns a single delay shared across all outgoing connections, leading to $\mathcal{O}(h)$ parameter scaling. In our formulation, up to n_d

delay parameters can be learned per neuron while maintaining the same $\mathcal{O}(h)$ scaling, which is significantly more efficient than the $\mathcal{O}(h^2)$ scaling of synaptic weights.

Memory The delay state $\mathbf{v}_d \in \mathbb{R}^{n_d \times 1}$ acts as a memory buffer storing n_d values per neuron. The intrinsic neuron state $\mathbf{v}_s \in \mathbb{R}^{n_s \times 1}$ already contains n_s internal variables. For example, the LIF neuron has one state variable (membrane potential), $n_s = 1$, while the adLIF includes an additional adaptation variable, giving $n_s = 2$. Appending \mathbf{v}_d to \mathbf{v}_s in (6) increases the number of state variables per neuron from n_s to $n_s + n_d$. At the network level, across l hidden layers with h neurons each, the total number of stored states grows from $n_s hl$ to $(n_s + n_d)hl$. However, since n_s , n_d , and l are typically much smaller than h (see Section 3.4), the overall memory footprint in both cases scales primarily with h .

4 Experimental Set-up

Network Architecture and Training In all experiments, a network with two hidden layers is used with batch normalization layers and an accumulative output layer with cross entropy loss. Each model is trained using BPTT with surrogate gradient [27]. We present further details for training and network parameters in Appendix A.4.

Dataset The Spiking Heidelberg Digits (SHD) dataset [5] consists of spike sequences derived from microphone recordings via the Lauscher cochlea model, covering 20 classes (digits 0-9 in German and English) across 8156 training and 2264 test samples, each with 700 input channels. The task is to classify the spoken digit from the input spike sequence. The Pre-processing details are in the Appendix A.5.

5 Results

We discuss the numerical experiments in Tables 2–5, covering comparisons to literature (Section 5.1), the effect of delay order, delay parameters, training time, and neuron count (Sections 5.2–5.5), and the effect of trainable vs. non-trainable delays (Section 5.6).

5.1 Comparison to literature

In this section, we compare our best performance presented in this paper with the performances of SHD dataset with other SNN works which include delays, see Table 2. We observe that our model is comparable both in terms of performance and in terms of number of parameters used.

Note that in general, the highest average accuracy reported over multiple initialization instances for the SHD dataset using SNNs is 95.07% [17], which is included in Table 2. The benchmark performance using a non-spiking encoding of the same data and a recurrent neural network is 99.69% [2].

Table 2: Accuracy and number of parameters reported for delay-based SNN papers on the SHD dataset. M denotes millions of parameters.

Paper	Accuracy	# params.
Learning DCLS [17]	95.07 \pm 0.24 %	0.2M
Co-learning [7]	95.02 %	0.076M
Learnable axonal delay [33]	93.55 %	0.21M
Event-based Delay [25]	93.24 \pm 1.00 %	0.5M ^(a)
Temporal Hierarchy [26]	92.1 % ^(b)	-
DMP [34]	91.69 %	0.046M
Heterogeneous Delays [32]	90.98 %	0.1M ^(c)
Ours (adLIF, $n_d = 5$, non-train. \mathbf{A}_{sd})	94.1 \pm 0.5 %	0.04M

^(a) Read from [25, Fig. 5];

^(b) Read from [26, Fig. 5];

^(c) Read from [32, Fig. 1c].

5.2 Order of delays

In this section, we discuss the varying order of delays i.e., we compare $n_d = 0, 5$ and 10, see Table 3.

We observe that increasing the delay order from $n_d = 0$ (i.e. no delay, hence the same as the traditional neuron types) to $n_d = 5$ or $n_d = 10$ either maintains or improves performance for LIF, adLIF, and RadLIF neurons. For example for \mathbf{A}_{sd} non-trainable, the adLIF baseline accuracy with $n_d = 0$ is $92.0 \pm 0.4\%$, while for $\mathbf{A}_{sd} = \text{Uniform}$ and $n_d = 5$ the accuracy rises to $94.1 \pm 0.5\%$, indicating an improvement beyond the standard deviation range. In contrast, RLIF neuron either maintains its performance or shows only a slight decrease when delays are introduced. For example, for \mathbf{A}_{sd} non-trainable, RLIF baseline accuracy with $n_d = 0$ is $90.6 \pm 0.5\%$, while for $\mathbf{A}_{sd} = \text{Ones}$ and $n_d = 5$ the accuracy drops to $87.7 \pm 1.1\%$, indicating a performance drop beyond the standard deviation range.

When comparing $n_d = 5$ and $n_d = 10$, the results remain within the standard deviation of each other, suggesting that increasing the delay order to $n_d = 10$ does not yield additional benefits beyond what $n_d = 5$ already captures.

Table 3: Test accuracy on the SHD dataset across combinations of neuron model, delay parameters \mathbf{A}_{sd} , and delay order n_d . All networks consist of two hidden layers with $h = 128$ neurons each. Bold indicates the best result per row.

(a) \mathbf{A}_{sd} is non-trainable.

Neuron Model	No delay	$\mathbf{A}_{sd} = \text{Ones}$		$\mathbf{A}_{sd} = \text{Lin. Decay}$		$\mathbf{A}_{sd} = \text{Exp. Decay}$		$\mathbf{A}_{sd} \sim \text{Uniform}$	
		$n_d = 5$	$n_d = 10$	$n_d = 5$	$n_d = 10$	$n_d = 5$	$n_d = 10$	$n_d = 5$	$n_d = 10$
LIF	85.9 \pm 1.2	86.6 \pm 1.2	83.8 \pm 2.0	86.6 \pm 0.8	85.9 \pm 0.8	86.7 \pm 0.7	86.0 \pm 0.9	87.2 \pm 1.6	86.7 \pm 0.8
RLIF	90.6 \pm 0.5	87.7 \pm 1.1	87.1 \pm 1.1	88.8 \pm 1.0	87.8 \pm 0.6	87.9 \pm 1.7	89.0 \pm 0.7	89.6 \pm 1.0	88.0 \pm 0.9
adLIF	92.0 \pm 0.4	92.1 \pm 0.2	91.6 \pm 0.4	93.3 \pm 0.9	91.8 \pm 0.8	93.3 \pm 0.4	93.0 \pm 0.9	94.1 \pm 0.5	92.1 \pm 1.3
RadLIF	93.4 \pm 1.1	91.6 \pm 2.6	91.2 \pm 2.2	92.8 \pm 0.7	92.4 \pm 0.9	93.8 \pm 0.6	93.5 \pm 0.4	93.1 \pm 1.2	92.1 \pm 1.2

(b) \mathbf{A}_{sd} is trainable.

Neuron Model		$\mathbf{A}_{sd} = \text{Ones init.}$		$\mathbf{A}_{sd} = \text{Lin. Decay init.}$		$\mathbf{A}_{sd} = \text{Exp. Decay init.}$		$\mathbf{A}_{sd} \sim \text{Uniform init.}$	
		$n_d = 5$	$n_d = 10$	$n_d = 5$	$n_d = 10$	$n_d = 5$	$n_d = 10$	$n_d = 5$	$n_d = 10$
LIF	—	87.7 \pm 0.9	88.2 \pm 1.0	88.4 \pm 1.2	89.1 \pm 0.3	89.1 \pm 0.8	89.6 \pm 1.1	88.4 \pm 1.5	89.5 \pm 0.5
RLIF	—	88.5 \pm 1.7	87.9 \pm 1.3	89.0 \pm 0.5	89.5 \pm 1.2	89.1 \pm 0.6	90.3 \pm 0.9	88.9 \pm 0.5	89.7 \pm 0.8
adLIF	—	92.7 \pm 0.7	91.9 \pm 0.5	93.1 \pm 0.4	92.7 \pm 0.5	93.6 \pm 0.2	93.6 \pm 1.1	93.3 \pm 0.6	92.6 \pm 0.5
RadLIF	—	93.4 \pm 0.8	92.4 \pm 1.3	94.0 \pm 0.2	93.3 \pm 0.6	93.4 \pm 0.5	93.7 \pm 0.6	93.7 \pm 0.6	92.3 \pm 1.0

5.3 Delay parameters

In this section we investigate the impact of using various delay parameter settings for \mathbf{A}_{sd} . In particular, we explore $\mathbf{A}_{sd} = \text{Ones}$, Linear Decay, Exponential Decay, and $\mathbf{A}_{sd} \sim \text{Uniform}$, see Section 3.3 for more details of the setting. Table 3 provides the associated results.

No consistent trend for delay weight parametrization is observed across all n_d values and neuron types, with most accuracy values falling within one standard deviation of each other and remaining differences appearing model-specific. For instance, the adLIF neuron achieves its best non-trainable \mathbf{A}_{sd} performance with the Uniform setting, while the Exponential Decay initialization yields the highest accuracy in the trainable case.

5.4 Training time

In this section, we discuss the additional training time introduced by using delays on NVIDIA Tesla T4 GPU with 16GB RAM, see Table 4. We first focus on the increase in training time when using $n_d = 5$ compared to the baseline with no delay. The smallest ratio increase, $\frac{13.1}{8.6} = 1.5$, occurs for the adLIF model with a non-trainable \mathbf{A}_{sd} , while the largest, $\frac{12.5}{6.5} = 1.8$, is observed for the LIF model with a trainable \mathbf{A}_{sd} . Increasing n_d from 5 to 10 results in only a negligible change in training time.

Table 4: Training time in minutes as average over the various delay parameters \mathbf{A}_{sd} settings for fixed n_d from Table 3.

Neuron Model	No delay	\mathbf{A}_{sd} non-trainable		\mathbf{A}_{sd} trainable	
		$n_d = 5$	$n_d = 10$	$n_d = 5$	$n_d = 10$
LIF	6.5 ± 0.1	11.7 ± 0.1	12.0 ± 0.2	12.5 ± 0.2	12.7 ± 0.3
RLIF	7.9 ± 0.1	13.1 ± 0.2	12.9 ± 0.1	13.9 ± 0.2	13.7 ± 0.1
adLIF	8.6 ± 0.1	13.1 ± 0.3	13.4 ± 0.6	14.1 ± 0.2	13.9 ± 0.1
RadLIF	9.6 ± 0.1	15.4 ± 0.2	15.1 ± 0.1	15.9 ± 0.4	16.0 ± 0.3

5.5 Number of neurons vs order of delays

In this section, we discuss the combined effect of the number of neurons in the hidden layers h and the order of delays n_d , see Table 5. The impact of increasing n_d on the performance depends on the number of neurons h . For $h \geq 32$, using delays ($n_d = 10, 50$ or 100) maintains performance at a level similar to no-delay or slightly reduces it. In contrast, for smaller networks with $h \leq 16$, using delays yields a clear improvement over the baseline no-delay performance. Note that in our implementation, the input sequences of the SHD dataset have a length of 100. Consequently, $n_d = 100$ allows the network to access the entire temporal history of each sample at every time step.

5.6 Trainable vs non-trainable delay parameters

In this section, we compare results with trainable and non-trainable \mathbf{A}_{sd} matrices.

Table 5: Test accuracy on the SHD dataset across combinations of neuron count h and delay order n_d for adLIF neurons with $\mathbf{A}_{sd} \sim \text{Uniform}$. Bold indicates the best result per row.

h	No delay	\mathbf{A}_{sd} non-trainable			\mathbf{A}_{sd} trainable		
		$n_d = 10$	$n_d = 50$	$n_d = 100$	$n_d = 10$	$n_d = 50$	$n_d = 100$
512	92.5 \pm 0.7	92.7 \pm 0.9	90.8 \pm 1.5	90.4 \pm 1.0	93.6 \pm 0.3	92.2 \pm 0.8	92.7 \pm 0.9
256	93.1 \pm 1.1	92.1 \pm 0.5	90.6 \pm 1.3	89.9 \pm 0.6	93.4 \pm 0.6	92.2 \pm 0.7	91.7 \pm 1.2
128	92.0 \pm 0.4	92.1 \pm 1.3	89.8 \pm 1.2	89.4 \pm 0.6	92.6 \pm 0.5	92.3 \pm 0.5	91.9 \pm 1.0
64	91.3 \pm 1.1	91.8 \pm 1.3	89.6 \pm 1.1	89.4 \pm 1.8	92.7 \pm 1.1	91.9 \pm 1.0	91.5 \pm 1.0
32	88.7 \pm 2.2	90.2 \pm 1.3	86.8 \pm 1.4	88.2 \pm 1.2	90.5 \pm 1.3	90.5 \pm 0.8	90.4 \pm 0.9
16	78.1 \pm 1.0	86.2 \pm 1.0	84.1 \pm 1.2	83.0 \pm 1.0	86.9 \pm 1.2	86.6 \pm 0.7	87.1 \pm 1.2
8	60.1 \pm 7.4	72.6 \pm 2.5	70.1 \pm 2.6	73.8 \pm 1.9	75.3 \pm 1.6	77.3 \pm 2.2	80.3 \pm 1.3

Tables 3a and 3b show that the accuracy values are generally within one standard deviation of each other, except for the LIF case where trainable \mathbf{A}_{sd} provides a clear benefit. Similarly, Table 5 shows no meaningful difference for $h \geq 32$. In contrast, for smaller networks ($h \leq 16$), the difference can be significant, for example, at $h = 8$ and $n_d = 100$, trainable \mathbf{A}_{sd} improves accuracy from 73.8% to 80.3%.

Table 4 shows that the additional training time for trainable \mathbf{A}_{sd} is negligible (< 1 min), further supporting the low computational overhead discussed in Section 3.4.

6 Discussions

The limited state dimensionality of LIF and adLIF neurons may restrict their ability to fully exploit the proposed delay mechanism; richer neuron models with more internal dynamics could deliver further benefits. No dedicated hyperparameter optimization (HPO) was performed, which could further improve performance and alter observations. Finally, whether the proposed delay neuron models can be efficiently implemented on neuromorphic hardware, as has been explored for some mechanisms [16], remains an open question.

7 Conclusion

In this work, we propose a general framework for incorporating delays into spiking neuron dynamics by introducing additional state variables that encode a finite temporal history, enabling seamless integration with a wide range of neuron models. We analyze the effect of delay order, trainable versus fixed delay parameters, and the trade-off between delay order and network size. The results show that the proposed mechanism achieves performance comparable to existing delay-based approaches while introducing minimal additional trainable parameters or not at all.

Acknowledgments. S. Karilanova and A. Özçelikkale acknowledge the support of Center for Interdisciplinary Mathematics (CIM), Uppsala University. The computations

were enabled by resources provided by the National Academic Infrastructure for Supercomputing in Sweden (NAISS), partially funded by the Swedish Research Council through grant agreement no. 2022-06725.

A Appendix

A.1 Proposed Method applied to LIF/AdLIF

LIF and RLIF example The discrete-time Leaky Integrate-and-Fire (LIF) neuron, as defined in [1], with the additional proposed delays is given by:

$$\mathbf{v}_d[t+1] = \mathbf{A}_d \mathbf{v}_d[t] + \mathbf{B}_d i_d[t] \quad (8a)$$

$$u[t+1] = \alpha u[t] + (1 - \alpha) i_s[t] - \alpha \theta s[t] + \mathbf{A}_{sd} \mathbf{v}_d[t] \quad (8b)$$

$$s[t] = f_\theta(u[t]) = \begin{cases} 1 & \text{if } u[t] \geq \theta \\ 0 & \text{otherwise.} \end{cases} \quad (8c)$$

where $i_s[t] = \mathbf{W} \times \mathbf{s}^{l-1}[t] + \mathbf{V} \times \mathbf{s}^l[t]$ for Recurrent LIF (RLIF) and $i_s[t] = \mathbf{W} \times \mathbf{s}^{l-1}[t]$ for LIF. For both RLIF and LIF, we have $i_d[t] = \mathbf{W} \times \mathbf{s}^{l-1}[t]$.

adLIF and RadLIF example The Adaptive Leaky Integrate-and-Fire (adLIF) neuron is an extension of the LIF neuron with an additional recovery state variable, $w[t]$ [1]. Discrete-time adLIF neuron with the additional proposed delays is:

$$\mathbf{v}_d[t+1] = \mathbf{A}_d \mathbf{v}_d[t] + \mathbf{B}_d i_d[t] \quad (9a)$$

$$u[t+1] = \alpha u[t] + (1 - \alpha) [i_s[t] - w[t]] - \alpha \theta s[t] + \mathbf{A}_{sd} \mathbf{v}_d[t+1] \quad (9b)$$

$$w[t+1] = \alpha w[t] + \beta w[t] + bs[t] \quad (9c)$$

$$s[t] = f_\theta(u[t]) = \begin{cases} 1 & \text{if } u[t] \geq \theta \\ 0 & \text{otherwise.} \end{cases} \quad (9d)$$

The inputs $i_s[t]$ and $i_d[t]$ are as defined for RLIF in Section A.1 with a correspondence between LIF and adLIF, and RLIF and Recurrent adLIF (RadLIF).

A.2 Linear SSM with Time Shift State Transition Matrix Demonstration

For the SSM state variable \mathbf{v}_d defined with Time Shift State Transition Matrix and initial state $\mathbf{v}_d[0] = \mathbf{0}^{n_d \times 1}$ we have:

$$\begin{aligned} \mathbf{v}_d[1] &= [i_d[1], 0, 0, \dots, 0]^T \\ \mathbf{v}_d[2] &= [i_d[2], a_1 i_d[1], 0, \dots, 0]^T \\ \mathbf{v}_d[3] &= [i_d[3], a_1 i_d[2], a_2 a_1 i_d[1], \dots, 0]^T \\ &\vdots \\ \mathbf{v}_d[t] &= [i_d[t], a_1 i_d[t-1], a_2 a_1 i_d[t-2], \dots, \\ &\quad \left(\prod_{k=1}^{n-1} a_k \right) i_d[t - n_d + 1]]^T. \end{aligned}$$

A.3 Delay parameters: temporal convolution representation

Under our parameter choices, the delay state $\mathbf{v}_d[t]$ stores the past n_d inputs $i_d[t]$. The term $\mathbf{A}_{sd} \mathbf{v}_d[t]$ therefore represents a weighted combination of these past inputs. Illustration shown in Figure 4.

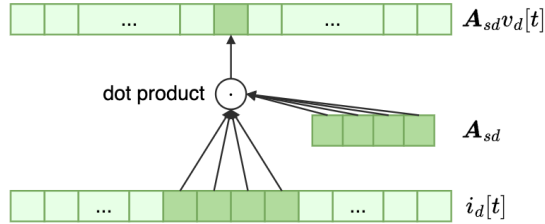


Fig. 4: Temporal convolution representation of the delay component. Under our parameter choices, the delay variable $\mathbf{v}_d[t]$ stores the past n_d inputs $i_d[t]$, hence the term $\mathbf{A}_{sd} \mathbf{v}_d[t]$ corresponds to a weighted combination of them.

A.4 Network and Training further details

Our code is based on the Sparch implementation [1]. During the training process, neuron parameters are clipped to remain within these boundaries as in [7] i.e. $\alpha \in [0.36, 0.96]$, $\beta \in [0.96, 0.99]$, $a \in [0, 1]$ and $b \in [0, 2]$. For training we use AdamW optimizer [23] and cosine learning rate scheduler. Batch normalization is used following [18].

We use hyperparameters based on previous works [7, 17, 29], in particular base LR = 10^{-2} , WD = 10^{-5} , dropout rate = 0.4, batch size = 128, and number of epochs = 50. No hyperparameter optimization has been performed.

A.5 Dataset further details

For the SHD dataset, similar to other works [17] [7] we used spatio-temporal bins to reduce the input dimensions. The input channels were reduced from 700 to 140 by binning every 5 consecutive channels.

The dataset was put in frames using the To-Frame [22] function with time-window= 10000, i.e. accumulation of events with time-windows of 10ms. The framed data set was used to load batches during both training and testing. During training, we use the data augmentation techniques `TimeNeurons_mask_aug` and `CutMix` following previous work [7] [17].

References

1. Bittar, A., Garner, P.N.: A surrogate gradient spiking baseline for speech command recognition. *Frontiers in Neuroscience* **16** (2022)
2. Boeshertz, G., Indiveri, G., Nair, M., Renner, A.: Accurate mapping of RNNs on neuromorphic hardware with adaptive spiking neurons. *ACM ICONS* (2024)
3. Carr, C.E., et al.: Processing of temporal information in the brain. *Annual review of neuroscience* **16**(1) (1993)
4. Carr, C., Konishi, M.: A circuit for detection of interaural time differences in the brain stem of the barn owl. *Journal of Neuroscience* **10**(10) (1990)
5. Cramer, B., Stradmann, Y., Schemmel, J., Zenke, F.: The heidelberg spiking data sets for the systematic evaluation of spiking neural networks. *IEEE Trans. on Neural Networks and Learning Systems* **33**(7) (2022)
6. Davies, M., Wild, A., Orchard, G., Sandamirskaya, Y., Guerra, G.A.F., Joshi, P., Plank, P., Risbud, S.R.: Advancing neuromorphic computing with Loihi: A survey of results and outlook. *Proceedings of the IEEE* **109**(5) (2021)
7. Deckers, L., Van Damme, L., Van Leekwijck, W., Tsang, I.J., Latré, S.: Co-learning synaptic delays, weights and adaptation in spiking neural networks. *Frontiers in Neuroscience* **18** (2024)
8. Diaz, C., Sanchez, G., Duchen, G., Nakano, M., Perez, H.: An efficient hardware implementation of a novel unary spiking neural network multiplier with variable dendritic delays. *Neurocomputing* **189** (2016)
9. Dominijanni, M., Ororbia, A., Regan, K.W.: Extending spike-timing dependent plasticity to learning synaptic delays. *arXiv:2506.14984* (2025)
10. Du, Y., Liu, X., Chua, Y.: Spiking structured state space model for monaural speech enhancement. In: *IEEE ICASSP* (2024)
11. Fu, D.Y., Dao, T., Saab, K.K., Thomas, A.W., Rudra, A., Ré, C.: Hungry hungry hippos: Towards language modeling with state space models. *ICLR* (2023)
12. Gajic, Z.: *Linear Dynamic Systems and Signals*. Prentice Hall - Pearson Education Inc. (2003)
13. Gallego, G., Delbrück, T., Orchard, G., Bartolozzi, C., Taba, B., Censi, A., Leutenegger, S., Davison, A.J., Conradt, J., Daniilidis, K., Scaramuzza, D.: Event-based vision: A survey. *IEEE Transactions on Pattern Analysis and Machine Intelligence* **44** (2022)
14. Grappolini, E., Subramoney, A.: Beyond weights: Deep learning in spiking neural networks with pure synaptic-delay training. In: *ACM ICONS 2023*. Association for Computing Machinery (2023)

15. Gu, A., Goel, K., Ré, C.: Efficiently modeling long sequences with structured state spaces. arXiv:2111.00396 (2022)
16. Göltz, J., Weber, J., Kriener, L., Billaudelle, S., Lake, P., Schemmel, J., Payvand, M., Petrovici, M.A.: Delgrad: exact event-based gradients for training delays and weights on spiking neuromorphic hardware. *Nature Communications* **16** (2025)
17. Hammouamri, I., Khalfaoui-Hassani, I., Masquelier, T.: Learning delays in spiking neural networks using dilated convolutions with learnable spacings. *ICLR* (2024)
18. Ioffe, S., Szegedy, C.: Batch normalization: accelerating deep network training by reducing internal covariate shift. In: *ICML*. vol. 37 (2015)
19. Karilanova, S., Dey, S., Özçelikkale, A.: State-space model inspired multiple-input multiple-output spiking neurons. In: *IEEE NICE* (2025)
20. Karilanova, S., Dey, S., Özçelikkale, A.: Low-bit data processing using multiple-output spiking neurons with non-linear reset feedback. *IEEE Journal of Selected Topics in Signal Processing* (2025)
21. Karilanova, S., Fabre, M., Neftci, E., Özçelikkale, A.: Zero-shot temporal resolution domain adaptation for spiking neural networks. *Neural Networks* (2025)
22. Lenz, G., Chaney, K., Shrestha, S.B., Oubari, O., Picaud, S., Zarrella, G.: Tonic: event-based datasets and transformations. (2021), <https://tonic.readthedocs.io>
23. Loshchilov, I., Hutter, F.: Decoupled weight decay regularization. In: *ICLR* (2019)
24. Maass, W., Schmitt, M.: On the complexity of learning for spiking neurons with temporal coding. *Information and Computation* **153**(1) (1999)
25. Mészáros, B., Knight, J.C., Nowotny, T.: Efficient event-based delay learning in spiking neural networks. *Nature Communications* **16** (2025)
26. Moro, F., Aceituno, P.V., Kriener, L., Payvand, M.: The role of temporal hierarchy in spiking neural networks. arXiv:2407.18838 (2024)
27. Neftci, E.O., Mostafa, H., Zenke, F.: Surrogate gradient learning in spiking neural networks: Bringing the power of gradient-based optimization to spiking neural networks. *IEEE Signal Process. Magazine* **36** (2019)
28. Richard, J.P.: Time-delay systems: an overview of some recent advances and open problems. *Automatica* **39**(10) (2003)
29. Schöne, M., Sushma, N.M., Zhuge, J., Mayr, C., Subramoney, A., Kappel, D.: Scalable event-by-event processing of neuromorphic sensory signals with deep state-space models. *IEEE/ACM International Conference on Neuromorphic Systems (ICONS)* (2024)
30. Sename, O., Keqin, G., Vladimir L., K., Jie, C.: *Stability of time-delay systems*. Birkhäuser Boston, MA (2003)
31. Shrestha, S.B., Orchard, G.: Slayer: Spike layer error reassignment in time. *NeurIPS* **31** (2018)
32. Sun, P., Achterberg, J., Su, Z., Goodman, D.F.M., Akarca, D.: Exploiting heterogeneous delays for efficient computation in low-bit neural networks. arXiv:2510.27434 (2025)
33. Sun, P., Chua, Y., Devos, P., Botteldooren, D.: Learnable axonal delay in spiking neural networks improves spoken word recognition. *Frontiers in Neuroscience* **17** (2023)
34. Sun, P., Su, Z., Achterberg, J., Indiveri, G., Goodman, D.F., Akarca, D.: Algorithm-hardware co-design of neuromorphic networks with dual memory pathways. arXiv preprint arXiv:2512.07602 (2025)
35. Vincent-Lamarre, P., Calderini, M., Thivierge, J.P.: Learning long temporal sequences in spiking networks by multiplexing neural oscillations. *Frontiers in Computational Neuroscience* **14** (2020)

36. Zhang, M., Saab, K.K., Poli, M., Dao, T., Goel, K., Ré, C.: Effectively modeling time series with simple discrete state spaces. ICLR (2023)